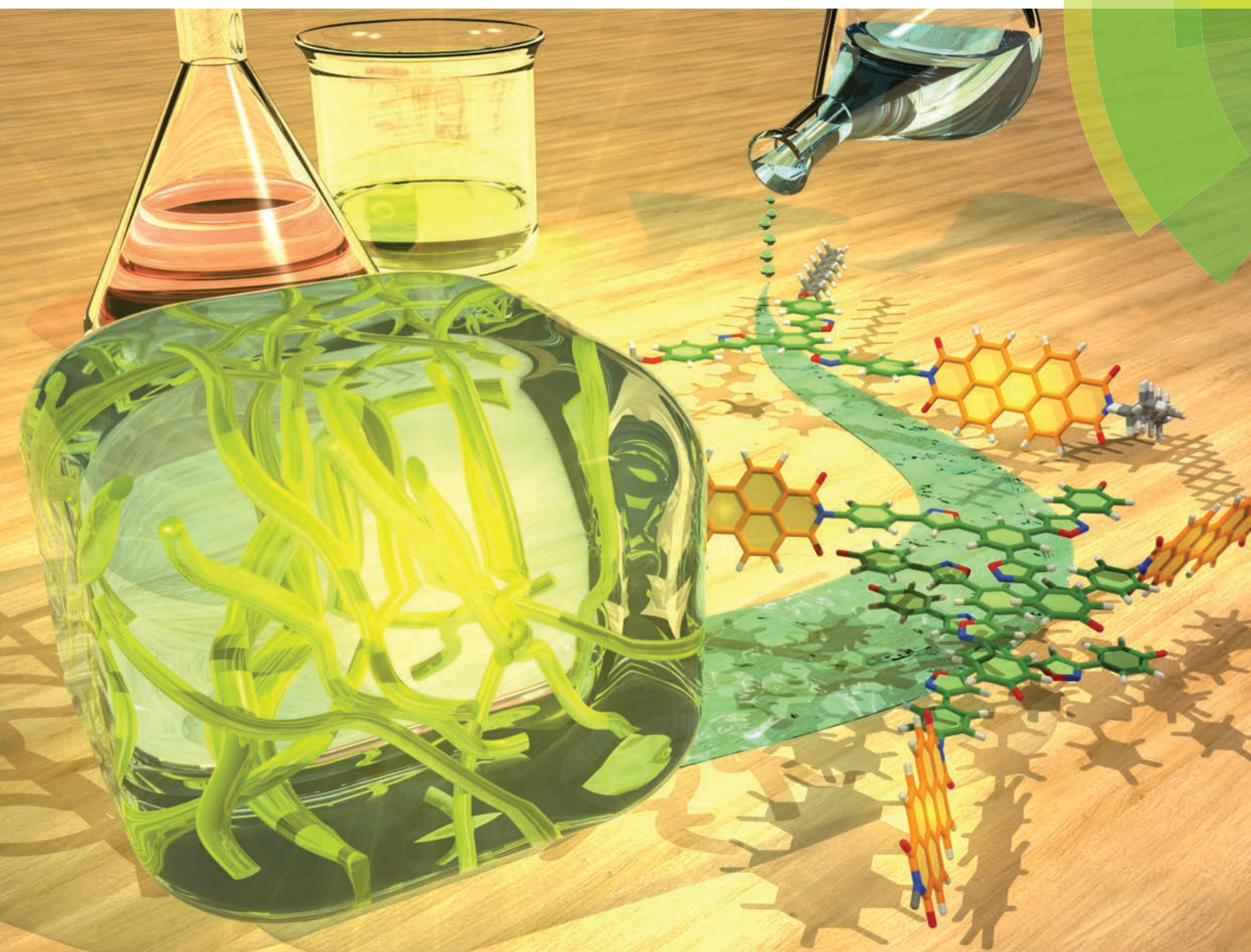


Organic & Biomolecular Chemistry

www.rsc.org/obc



ISSN 1477-0520



COMMUNICATION

Takeharu Haino *et al.*

Solvent-induced emission of organogels based on tris(phenylisoxazolyl) benzene

175 YEARS



Cite this: *Org. Biomol. Chem.*, 2016, **14**, 36

Received 12th September 2015,
Accepted 28th October 2015

DOI: 10.1039/c5ob01898f

www.rsc.org/obc

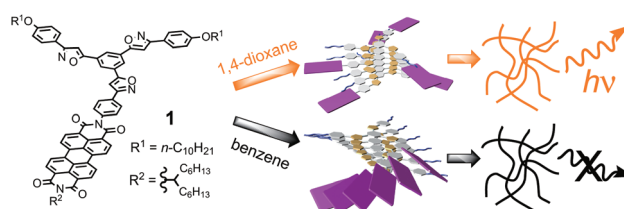
Solvent-induced emission of organogels based on tris(phenylisoxazolyl)benzene†

Toshiaki Ikeda, Tetsuya Masuda, Midori Takayama, Hiroaki Adachi and Takeharu Haino*

Luminescent organogels based on tris(phenylisoxazolyl)benzene possessing perylenebisimide **1 were synthesized. The emission properties of the gels varied depending on the solvent properties: 1,4-dioxane gel was highly emissive, pyridine gel was moderately emissive, and benzene gel was non-emissive.**

Strong emissions in condensed phases, such as solid,¹ liquid crystalline,² and gel,³ are indispensable because of their practical applications for luminescent materials. However, most planar aromatic dyes display weak emissions in the condensed phase because of inter-dye interactions. This is known as aggregation-caused quenching (ACQ).⁴ Many research groups have made numerous efforts to overcome ACQ.^{5,6} The most important factor for mitigating ACQ is pulling the dyes away from each other in their condensed phase. One way to achieve this is to separate the dye and the assembling moiety, which leads to the formation of an assembly in which the dyes are not close to each other.

Recently, our group has developed the self-assembly of tris(phenylisoxazolyl)benzenes.⁷ The molecules form helical stacked assemblies *via* π - π stacking and intermolecular dipole-dipole interactions of the isoxazole and are good low molecular-weight organogelators (LMOG).^{7c,e-g} The introduction of dyes onto the tris(phenylisoxazolyl)benzenes produced photo-functional assemblies.^{7a,d} Herein, we report a fluorescent organogel fabricated by tris(phenylisoxazolyl)benzene possessing perylenebisimide (PBI) and long alkyl side-chains, **1** (Scheme 1). This molecule forms stacked assemblies and gels in various solvents, but the structure of the assembly varies depending on the solvent properties. Interestingly, the gel of 1,4-dioxane showed strong fluorescence, whereas the gels of other solvents displayed weak or no fluorescence.



Scheme 1 Chemical structure of **1** and schematic representation of the assemblies and gels.

The gelation behaviors of **1** were examined using the “inverted test-tube method”. **1** and solvents were placed into a capped test tube and heated until the solid dissolved. The solution was sonicated for several minutes and then cooled to 298 K and left for 2 h under ambient conditions. Gelation was confirmed by the absence of the gravitational flow of solvents when the test tube was inverted (Table 1). The gels were thermo-reversible and stable for at least 1 month at room temperature. **1** gelled cyclic hydrocarbons, cyclic ethers, and aromatic solvents. The colors and emission properties of the gels depended on the solvent properties. **1** formed yellow gels in 1,4-dioxane and reddish-orange gels in pyridine and in THF, whereas the other solvents created dark red gels (Fig. S1†). The emissions of the gels differed substantially depending on the solvent properties: the 1,4-dioxane gel showed strong yellow fluorescence, the pyridine and THF gels showed moderate red fluorescence, and the other gels showed no emissions (Fig. S2†). The variation of the color and emissions of the gels can be controlled by the assembly structure in the gel phase.

The UV-vis absorption and fluorescence spectra of the solutions and gels of **1** provided further insight into the assembly structures. Fig. 1c displays the absorption spectra of **1** in both 1,4-dioxane and decalin. The 1,4-dioxane solution of **1** produced a sharp visible absorption band with three vibrational structures (455, 485, and 521 nm), indicating that the monomeric form was dominant. In contrast, **1** displayed *J*-aggregation in decalin upon increasing a solution concentration of **1**,

Department of Chemistry, Graduate School of Science, Hiroshima University, 1-3-1 Kagamiyama, Higashi-Hiroshima, 739-8526, Japan.

E-mail: haino@hiroshima-u.ac.jp; Fax: +81 82 424 0724; Tel: +81 82 424 7427

† Electronic supplementary information (ESI) available: Synthetic procedure of **1**, photographs of gels, ¹H NMR, UV/vis absorption, and fluorescence spectra of **1** in solution, and NMR spectra of all new compounds. See DOI: 10.1039/c5ob01898f



Table 1 Gelation properties of **1**^{a,b,c}

Solvent		Solvent	
<i>n</i> -Hexane	I	Benzene	G(10)
<i>n</i> -Decane	I	Toluene	S
Cyclohexane	G(25)	Chlorobenzene	S
MCH	G(30)	<i>o</i> -Xylene	S
Decalin	S	<i>o</i> -Dichlorobenzene	G(30)
Acetone	I	1,2,4-Trimethylbenzene	S
Ethyl acetate	I	1,2,4-Trichlorobenzene	S
DMF	P	Pyridine	G(10)
DMSO	I	4-Methylpyridine	G(25)
Triethylamine	S	Benzonitrile	G(30)
Diisopropylamine	P	Acetonitrile	I
Methanol	I	Diethyl ether	S
Ethanol	I	THF	G(20)
2-Propanol	I	1,4-Dioxane	G(3)
Decanol	I	Dichloromethane	S
Benzyl alcohol	I	Chloroform	S
<i>p</i> -Cresol	S		

^a G = gel, P = precipitation, S = solution, and I = insoluble. ^b P, I, and S are at [1] = 20 g L⁻¹. ^c The critical gelation concentration (g L⁻¹) is shown in parentheses.

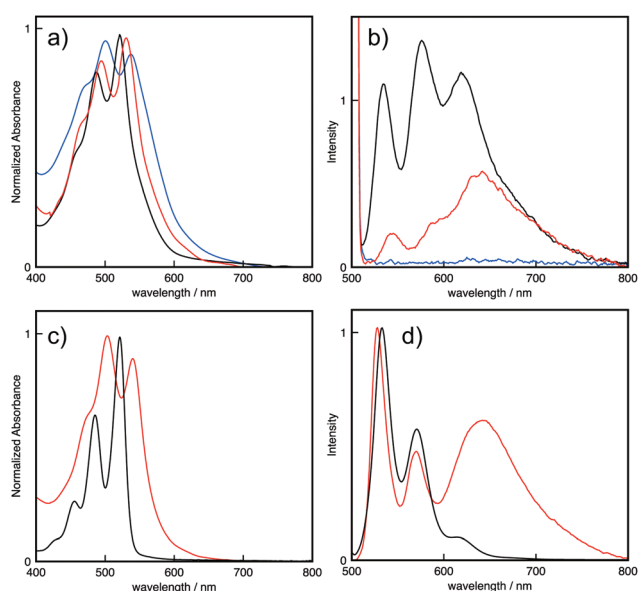


Fig. 1 (a) UV-vis absorption and (b) emission spectra of **1** in 1,4-dioxane gel (black line), in pyridine gel (red line), and in benzene gel (blue line). (c) UV-vis absorption and (d) emission spectra of **1** in 1,4-dioxane solution (black line) and decalin solution (red line) at 25 °C. [1] = 1.0 × 10⁻⁵ mol L⁻¹. λ_{ex} = 500 nm.

resulting in red-shifts of the visible absorption band (471, 502, and 540 nm).^{7d,8} The absorption spectra of **1** in the gel phase show the characteristics of the assembling behaviors, which are controlled by the solvent properties. The UV-vis absorption spectrum of the 1,4-dioxane gel of **1** (Fig. 1a, black line, λ_{max} = 460, 487, and 521 nm) resembles that of the monomeric species. Thus, most of the PBI moieties do not form *J*-aggregates in the 1,4-dioxane gel. In contrast, the benzene gel

showed a bathochromic shift. The λ_{max} values of the benzene gel (471, 501, and 538 nm) are almost the same as those of the *J*-aggregates in decalin solution, suggesting the formation of a *J*-aggregate in the benzene gel (Fig. 1a, blue line). The pyridine gel showed red-shifted absorptions (465, 495, and 530 nm) smaller than those in the benzene gel. Therefore, the monomeric form and aggregated form of **1** coexisted, even in the gel phase.

1 displayed the sharp fluorescence of the monomeric PBI with a high quantum yield (φ = 0.78) in 1,4-dioxane solution (Fig. 1d, black line). In decalin solution, **1** showed a broad and red-shifted fluorescence of the *J*-aggregated PBI (Fig. 1d, red line).^{7d,8} The quantum yield in decalin solution was low (φ = 0.060) because of ACQ. The fluorescence spectrum of the highly fluorescent 1,4-dioxane gel is quite similar to that in 1,4-dioxane solution, while the spectrum contains weak emission of the *J*-aggregates at 620 nm (Fig. 1b, black line). The pyridine gel showed aggregated fluorescence as well as very weak monomeric emission (Fig. 1b, red line), whereas the benzene gel exhibited no emission (Fig. 1b, blue line). The quantum yield of 1,4-dioxane gel is 0.066, which is higher than that of the pyridine gel (φ = 0.035). These results support the same conclusion as the absorption spectra: the solvent properties drive the aggregation behavior of **1**.

To obtain insight into the assembly structure, ¹H NMR spectroscopy was employed. The ¹H NMR signals of **1** were concentration dependent in chloroform-*d*₁ (Fig. 2). Most of the aromatic signals shifted upfield as the concentration increased from 0.063 to 8.0 mmol L⁻¹. Thus, these molecules form stacked assemblies in which the aromatic protons are located in the shielding regions produced by the neighboring molecules. Plotting the chemical shift changes of the protons vs. the concentrations of **1** produced hyperbolic curves. Non-linear curve-fitting analysis by applying the isodesmic model produced estimated complexation-induced shifts (Δδ = -0.29, -0.64, -0.31, -1.13, -0.79, -0.33, -0.33, -0.33, and -0.43 ppm for H_a, H_b, H_c, H_d, H_e, H_f, H_g, H_h, and H_{PBI}, respectively) and the association constant (K_E = 24 ± 6 L mol⁻¹). The characteristic upfield shifts of the aromatic protons

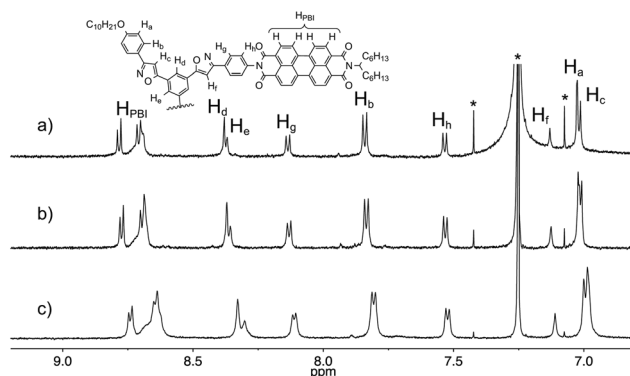


Fig. 2 Concentration-dependent ¹H NMR spectra of **1** in chloroform-*d*₁. The concentrations are (a) 0.25, (b) 1.0, and (c) 4.1 mmol L⁻¹.



of H_c , H_d , H_e , and H_{PBI} imply that the molecules stack in piles around the pseudo C_3 axis on the tris(phenylisoxazolyl)benzene and that the peripheral substituent PBI creates a close contact with its neighbors. The 1H NMR spectra of **1** in benzene- d_6 , pyridine- d_5 , and 1,4-dioxane- d_8 were temperature dependent (Fig. S6–8†), and the aromatic signals broadened as the temperature decreased. This behavior indicates the formation of large aggregates in these solvents.

The morphologies of the xerogels of **1** were observed using field-emission scanning electron microscopy (FE-SEM). The gel morphology depended on the solvent properties. The xerogel of **1** obtained from the 1,4-dioxane gel displayed a highly entangled fibrous structure with voids (Fig. 3a). The xerogel obtained from the pyridine gel contains both fibrils and particles (Fig. 3b), while that obtained from the benzene gel exhibited stacked film-like aggregates with no fibrils observed (Fig. 3c).

Atomic force microscopy (AFM) observations of **1** on mica provided additional insight into the nano-scale morphology of the assemblies in the solid state. The assembly in benzene solution gave rise to well-developed fibers with an average height of 2.6 nm (Fig. 4d). The values closely matched the approximate molecular diameter of 2.9 nm for **1** without an alkyl side-chain, indicating that **1** stacked in a columnar fashion to form fibrillar bundles on the mica surface. In contrast, spin-coated films from pyridine and 1,4-dioxane solutions provided sheet-like morphologies with an average height of 3.4 nm (Fig. 4a and c). A magnified image of a spin-coated film of 1,4-dioxane solution shows parallel-arranged fibers (Fig. 4b). These results suggest that the assemblies of **1** in pyridine and 1,4-dioxane formed fibers that were bundled into sheet-like morphologies.

In conclusion, we have elucidated the gelation and emission properties of **1** in various solvents. **1** gelled cyclic hydro-

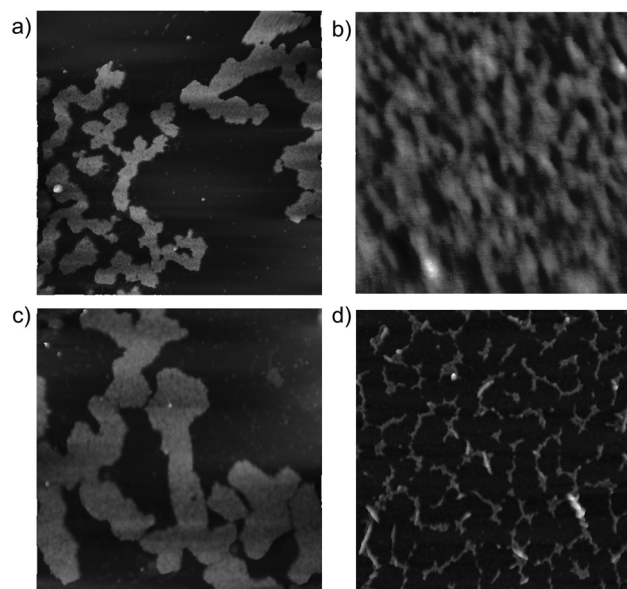


Fig. 4 AFM images of **1** spin-coated on mica. The solvents are (a, b) 1,4-dioxane, (c) pyridine, and (d) benzene. The sizes of the images are (a, c, d) $3.0\ \mu\text{m} \times 3.0\ \mu\text{m}$ and (b) $0.3\ \mu\text{m} \times 0.3\ \mu\text{m}$.

carbons, cyclic ethers, and aromatic solvents. The emission properties of the gels depended on the solvent properties. **1** displayed no emission in the benzene gel, weak emission in the pyridine gel, and strong emission in the 1,4-dioxane gel. The emission properties of **1** in these gels reflect the stacking structure of **1**. In the benzene gel, the PBI moiety of **1** formed stacked *J*-aggregates, which quench the fluorescence of **1**. In the 1,4-dioxane gel, the PBI moiety does not stack, and as a result, no fluorescence quenching occurs. The PBI moiety may be preferably solvated with 1,4-dioxane, preventing the *J*-aggregation, which results in the luminescence of the 1,4-dioxane gel.

Acknowledgements

This work was supported by Grants-in-Aid for Scientific Research (B) (No. 15H03817), Grants-in-Aid for Scientific Research (C) (No. 15KT0145), and Grants-in Aid for Young Scientists (B) (No. 26810051) of JSPS, as well as Grants-in-Aid for Scientific Research on Innovative Areas, “Stimuli-responsive Chemical Species for Creation of Functional Molecules” and “New Polymeric Materials Based on Element-Blocks” (No. 15H00946, 15H00752).

Notes and references

- (a) J. Mei, Y. Hong, J. W. Y. Lam, A. Qin, Y. Tang and B. Z. Tang, *Adv. Mater.*, 2014, **26**, 5429; (b) Y. S. Zhao, H. Fu, A. Peng, Y. Ma, Q. Liao and J. Yao, *Acc. Chem. Res.*, 2010, **43**, 409; (c) Y. Sagara and T. Kato, *Nat. Chem.*, 2009, **1**, 605;

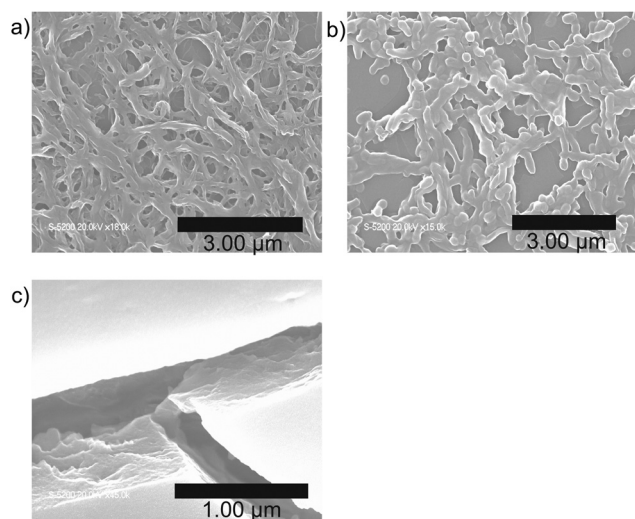


Fig. 3 SEM images of xerogels of **1**. (a) 1,4-Dioxane gel, (b) pyridine gel, and (c) benzene gel.



- (d) B. W. D'andrade and S. R. Forrest, *Adv. Mater.*, 2004, **16**, 1585.
- 2 (a) M. O'Neill and S. M. Kelly, *Adv. Mater.*, 2003, **15**, 1135; (b) D. Neher, *Macromol. Rapid Commun.*, 2001, **22**, 1365.
- 3 (a) S. S. Babu, V. K. Praveen and A. Ajayaghosh, *Chem. Rev.*, 2014, **114**, 1973; (b) T. Cardolaccia, Y. Li and K. S. Schanze, *J. Am. Chem. Soc.*, 2008, **130**, 2535; (c) F. Camerel, L. Bonardi, M. Schmutz and R. Ziessel, *J. Am. Chem. Soc.*, 2006, **128**, 4548; (d) A. Kishimura, T. Yamashita and T. Aida, *J. Am. Chem. Soc.*, 2005, **127**, 179; (e) S. Y. Ryu, S. Kim, J. Seo, Y.-W. Kim, O.-H. Kwon, D.-J. Jang and S. Y. Park, *Chem. Commun.*, 2004, 70; (f) B.-K. An, D.-S. Lee, J.-S. Lee, Y.-S. Park, H.-S. Song and S. Y. Park, *J. Am. Chem. Soc.*, 2004, **126**, 10232.
- 4 (a) W. Z. Yuan, P. Lu, S. M. Chen, J. W. Y. Lam, Z. M. Wang, Y. Liu, H. S. Kwok, Y. G. Ma and B. Z. Tang, *Adv. Mater.*, 2010, **22**, 2159; (b) S. W. Thomas, G. D. Joly and T. M. Swager, *Chem. Rev.*, 2007, **107**, 1339.
- 5 (a) N. Kato, T. Sanji and M. Tanaka, *Chem. Lett.*, 2009, **38**, 1192; (b) M. J. Frampton, T. D. W. Claridge, G. Latini, S. Brovelli, F. Cacialli and H. L. Anderson, *Chem. Commun.*, 2008, 2797; (c) M. J. Frampton and H. L. Anderson, *Angew. Chem., Int. Ed.*, 2007, **46**, 1028.
- 6 (a) Y. Hong, J. W. Y. Lam and B. Z. Tang, *Chem. Soc. Rev.*, 2011, **40**, 5361; (b) Z. Zhao, S. Chen, X. Shen, F. Mahtab, Y. Yu, P. Lu, J. W. Y. Lam, H. S. Kwok and B. Z. Tang, *Chem. Commun.*, 2010, **46**, 686; (c) B.-K. An, S.-K. Kwon, S.-D. Jung and S. Y. Park, *J. Am. Chem. Soc.*, 2002, **124**, 14410.
- 7 (a) T. Ikeda, M. Takayama, J. Kumar, T. Kawai and T. Haino, *Dalton Trans.*, 2015, **44**, 13156; (b) T. Haino, Y. Ueda, T. Hirao, T. Ikeda and M. Tanaka, *Chem. Lett.*, 2014, **43**, 414; (c) T. Haino, Y. Hirai, T. Ikeda and H. Saito, *Org. Biomol. Chem.*, 2013, **11**, 4164; (d) T. Ikeda, T. Masuda, T. Hirao, J. Yuasa, H. Tsumatori, T. Kawai and T. Haino, *Chem. Commun.*, 2012, **48**, 6025; (e) M. Tanaka, T. Ikeda, J. Mack, N. Kobayashi and T. Haino, *J. Org. Chem.*, 2011, **76**, 5082; (f) T. Haino and H. Saito, *Synth. Met.*, 2009, **159**, 821; (g) T. Haino, M. Tanaka and Y. Fukazawa, *Chem. Commun.*, 2008, 468.
- 8 (a) T. E. Kaiser, V. Stepanenko and F. Würthner, *J. Am. Chem. Soc.*, 2009, **131**, 6719; (b) F. Würthner, C. Bauer, V. Stepanenko and S. Yagai, *Adv. Mater.*, 2008, **20**, 1695.

